Dual fluidized bed biomass gasification: Temperature variation using pure CO_2 as gasification agent

A.M. Mauerhofer[1*], S. Müller[1], F. Benedikt[1], J. Fuchs[1], A. Bartik[1], M. Hammerschmid[1], and H. Hofbauer[1]

1. TU Wien, Institute of Chemical, Environmental and Bioscience Engineering (ICEBE), Getreidemarkt 9/166, 1060 Vienna, Austria
*corresponding author, anna.mauerhofer@tuwien.ac.at

Abstract

In many industrial processes, the climate-damaging gas CO_2 is produced as undesired by-product. The dual fluidized bed biomass gasification technology offers the opportunity to solve this problem by using the produced CO_2 within the process as gasification agent. Therefore, a 100 kW pilot plant at TU Wien was used to investigate the use of CO_2 as gasification agent by converting softwood as fuel and olivine as bed material into a product gas. A temperature variation from 740 to 840°C was conducted to investigate the change of the main product gas components over the gasification temperature. With increasing temperature, CO and H_2 increased and CO_2 decreased. Additionally, another parameter variation was conducted, where the typically used gasification agent steam was substituted stepwise by CO_2. Thereby, the amount of CO and CO_2 increased and the content of H_2 decreased. These trends resulted in a declining H_2/CO ratio and a decreasing lower heating value when CO_2 was increased as gasification agent.

1. Introduction

The increasing visible and noticeable effects of the climate change, require the development of efficient and feasible strategies to be able to meet the targets of the Paris Agreement. To achieve these targets, the research on efficient energy technologies with low greenhouse gas emissions and the possibility to recycle undesired by-products within the process is urgent. A possible technology could be the thermochemical conversion process of biomass gasification. In this way, fossil energy sources like crude oil or lignite are substituted by renewable, alternative feedstock to produce a highly- valuable product gas. This product gas could be further upgraded in different synthesis processes to produce fuels or other chemicals [1], [2]. Additionally, the recycling of produced carbon dioxide (CO_2) within the gasification process could reduce greenhouse gas emissions and contribute to the overall carbon cycle in a positive way. The dual fluidized bed (DFB) biomass gasification using steam as gasification agent has been developed successfully for more than 20 years at TU Wien [3]. However, the use of CO_2 as gasification agent presents a novel research topic at TU Wien. In contrast to pure steam biomass gasification, where a hydrogen (H_2)-enriched product gas is generated, a carbon monoxide (CO)-rich product gas is created, when CO_2 is used as gasification agent. In this way, the H_2/CO ratio, which presents an important factor for different synthesis processes, is influenced. With the DFB biomass gasification system, the adjustment of the H_2/CO ratio in a range of 0.6:1 to 10:1 is

possible [4], [5]. This presents a huge flexibility in the generation of the product gas for different synthesis processes.
In this publication, the influence of the gasification temperature on pure CO_2 as gasification agent is investigated. Additionally, a second parameter variation, the stepwise substitution of steam by CO_2 as gasification is discussed.

2. Concept and methodology

2.1 DFB CO_2/steam gasification reactor system

For the experimental test campaigns, a 100 kW_{th} DFB pilot plant, which was built at TU Wien, was used. The principle of the DFB gasification pilot plant is shown in **Fig. 1**. The pilot plant is composed of two reactors: a gasification reactor (GR, blue rectangle) and a combustion reactor (CR, red rectangle), which are connected by loop seals (horizontal arrows). The GR is divided in a lower part, where the devolatilization and gasification reactions take place and an upper part, where reforming and gasification reactions occur.

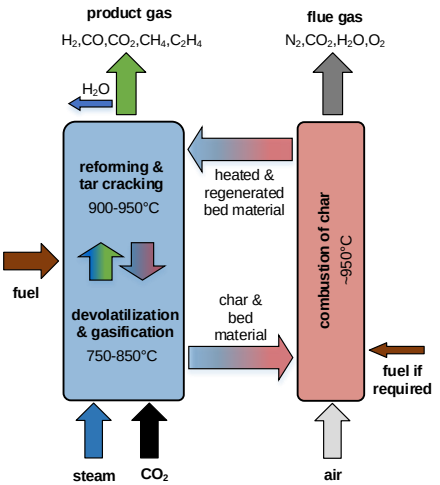

Fig. 1: Principle of the DFB CO_2/steam biomass gasification

The GR is fluidized with CO_2 and/or steam and the CR with air. Biomass is introduced into the GR. In the GR, a product gas, which is composed of CO, H_2, CO_2, methane (CH_4), ethylene (C_2H_4), water (H_2O) and other minor components, is generated. In the CR, a flue gas, which mainly contains CO_2, H_2O, nitrogen (N_2) and oxygen (O_2) is produced.

The 100 kW_{th} DFB biomass gasification pilot plant went into operation in 2014 [6]. **Fig. 2** shows the upper part of the pilot plant with three fuel hoppers and the lower part of the reactor system with some ash removal containers. The GR of the pilot plant is operated as bubbling bed in the lower part and as counter-current column with turbulent fluidized bed zones in the upper part. In the upper part of the gasification reactor, constrictions are implemented, which enable an increased interaction of hot bed material particles with the product gas. Thus, the residence time as well as the conversion efficiency is increased [7], [8].

Fig. 2: Upper part and lower part of the DFB biomass gasification system

2.2 Investigated materials

For the presented test campaigns, softwood (SW) pellets were used as fuel and olivine as bed material. The proximate and ultimate analysis of SW is shown in **Tab. 1** and the composition of olivine is presented in **Tab. 2**. Olivine was used as bed material because it is known as state-of-the-art bed material and is typically used in industrial-sized biomass gasification plants [9].

Tab. 1: Proximate and ultimate analysis of softwood pellets

parameter	unit	value
proximate analysis		
water content	wt.-%	7.2
volatiles	wt.-%$_{db}$	85.4
fixed C	wt.-%$_{db}$	14.6
LHV (dry)	MJ/kg$_{db}$	18.9
LHV (moist)	MJ/kg	17.4
ultimate analysis		
ash content	wt.-%$_{db}$	0.2
carbon (C)	wt.-%$_{db}$	50.7
hydrogen (H)	wt.-%$_{db}$	5.9
oxygen (O)	wt.-%$_{db}$	43.0
nitrogen (N)	wt.-%$_{db}$	0.2
sulphur (S)	wt.-%$_{db}$	0.005
chloride (Cl)	wt.-%$_{db}$	0.005
ash content	wt.-%$_{db}$	0.2
carbon (C)	wt.-%$_{db}$	50.7
ash melting behaviour		
deformation temperature (A)	°C	1335

Tab. 2: Composition of olivine

parameter	unit	value
Fe_2O_3	wt.-%	8.0 - 10.5
MgO	wt.-%	48 - 50
SiO_2	wt.-%	39 - 42
CaO	wt.-%	≤ 0.4
trace elements (< 0.4 per element)	wt.-%	≤ 4.6
hardness	Mohs	6 - 7
sauter mean diameter	mm	0.243
particle density	kg/m³	2850

2.3 Validation of process data with IPSE

To close the mass and energy balances of the experimental data recorded during the presented test campaigns, the software simulation tool IPSEpro was used. For this purpose, a detailed model library, which was developed at TU Wien over many years, was used. [10], [11]. The following key parameters were selected to describe the operation of the presented test campaigns. All input and output streams, which were used for the calculation of the key parameters are presented in **Fig. 3**. The carbon to CO conversion $X_{C\rightarrow CO}$ describes the amount of CO in the product gas to the total amount of introduced C as fuel and gasification agent (see **Eq. 1**). **Eq. 2** shows the CO_2 conversion rate X_{CO2}, which gives the ratio of consumed CO_2 during gasification to the amount of CO_2 introduced into the GR. Detailed information about the calculation of X_{CO2} can be found in [12]. X_{H2O} is defined as the steam-related water conversion. It presents water consumed for e.g. CO and H_2 production in relation to the sum of water, which is fed to the GR as gasification agent and fuel water (see **Eq. 3**). To describe the efficiency of the test campaigns, the overall cold gas efficiency $\eta_{CG,o}$ is given in **Eq. 4**. It shows the amount of chemical energy in the product gas in relation to the fuel introduced into the gasification and combustion reactor minus appearing heat losses.

$$X_{C\rightarrow CO} = \frac{x_{CO,PG} \times \dot{m}_{PG}}{x_{C,fuel} \times \dot{m}_{fuel,db} + x_{C,CO2,fluid} \times \dot{m}_{CO2,fluid}} \quad (1)$$

$$X_{CO_2} = \frac{\dot{m}_{CO2,fluid} + k_{CO2} \times \dot{m}_{fuel,daf} - x_{CO2,PG} \times \dot{m}_{PG}}{\dot{m}_{CO2,fluid} + \dot{m}_{fuel,daf} \times k_{CO2}} \quad (2)$$

$$X_{H2O} = \frac{\dot{m}_{steam} + x_{H2O,fuel} \times \dot{m}_{fuel} - x_{H2O,PG} \times \dot{m}_{PG}}{\dot{m}_{steam} + x_{H2O,fuel} \times \dot{m}_{fuel}} \quad (3)$$

$$\eta_{CG,o} = \frac{\dot{V}_{PG} \times LHV_{PG}}{\dot{m}_{GR,fuel} \times LHV_{GR,fuel} + \dot{m}_{CR,fuel} \times LHV_{CR,fuel} - \dot{Q}_{loss}} \cdot 100 \quad (4)$$

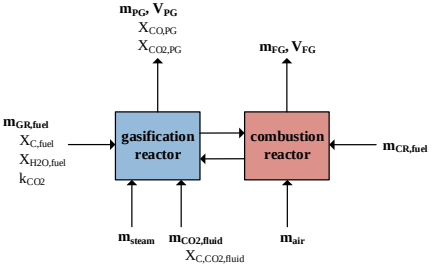

Fig. 3: Input and output streams for the calculation of the key parameters

In **Eq. 5**, a very important gasification reaction, namely the reverse water gas shift (RWGS) reaction, is shown and used for the discussion of the results. Additionally, the deviation of this reaction from thermodynamic equilibrium is shown in **Eq. 6**. The RWGS reaction is a homogeneous gas-gas reaction, which favors the CO production. The equilibrium constant $K_{p,RWGS}(T)$ was calculated using the software tool HSC [13]. If the deviation is zero, it means that the equilibrium state of the equation is reached. A negative value would indicate, that the gas composition is on the side of the reactants, which would mean, that a further reaction is thermodynamically possible. A positive sign would imply that the actual state is on the side of the products. However, this state can not be reached thermodynamically through the RWGS reaction alone. Additional reactions are required as stated in [14].

$$CO_2 + H_2 \rightleftharpoons CO + H_2O \quad (5)$$

$$p\delta_{eq,RWGS} = \log_{10}\left[\frac{\prod_i p_i^{\nu_i}}{K_{p,RWGS}(T)}\right] \quad (6)$$

2.4 Thermodynamic calculations

To compare the experimental results with theory, thermodynamic calculations were carried out beforehand. Therefore, the product gas compositions were calculated in their thermodynamic equilibrium with the software tool HSC Chemistry [13] based on the minimization of the Gibbs free energy. At the equilibrium state, the Gibbs free energy of the investigated system was minimized, which is explained in detail in [15].

3. Results and discussion

In **Tab. 3**, the main operational parameters of 5 test campaigns are shown. In these 5 test campaigns, the gasification agent was changed from pure H_2O to pure CO_2. Softwood was used as fuel and olivine as bed material for all test campaigns. The CO_2/H_2O ratio of the gasification agent was changed from 0/100 to 100/0 vol.-% in five steps. The temperatures in the gasification and the combustion reactor were in the same range. In the following, the experimental results are presented. To compare the experimental results with theory, thermodynamic calculations were carried out beforehand.

Tab. 3: Main operational parameters

		test campaign				
parameter	**unit**	**1**	**2**	**3**	**4**	**5**
fuel	-	SW	SW	SW	SW	SW
bed material	-	olivine	olivine	olivine	olivine	olivine
CO_2/H_2O fluidization	vol.-%	0/100	32/68	45/55	68/32	100/0
fuel to GR	kW	95	92	86	87	83
fuel to CR	kW	68	59	53	53	56
T GR_{lower}	°C	827	833	838	838	837
T GR_{upper}	°C	935	936	938	934	947
T CR_{outlet}	°C	947	944	944	941	964

Fig. 4 shows the course of the main product gas components depending on the gasification agent in the thermodynamic equilibrium for the 5 test campaigns. In the thermodynamic equilibrium, the H_2 content decreased and the CO content increased. The CO_2 content showed an increasing trend as well, but decreased abrupt when 100 vol.-% CO_2 was theoretically used as gasification agent. CH_4 remained almost 0 vol.-%$_{db}$ for all operating points in the thermodynamic equilibrium.

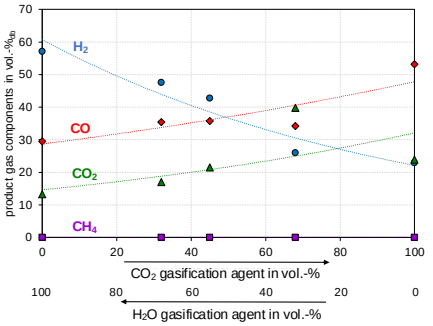

Fig. 4: Change of product gas composition over CO_2 input as gasification agent in the thermodynamic equilibrium

Fig. 5 presents the experimental results of the 5 test campaigns, where steam was substituted stepwise by CO_2.

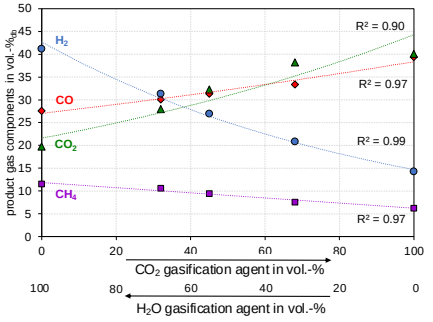

Fig. 5: Change of product gas composition over CO_2 input as gasification agent

CO_2 and CO showed an increasing trend with increasing CO_2 content as gasification agent. The opposite phenomenon was seen for H_2, which was decreasing with increasing CO_2 input. CH_4 slightly declined, but remained relatively stable. However, this declining trend could also be an effect of dilution. The best fitting trend lines with quite high coefficients of determination were calculated for H_2, CO and CO_2 with an exponential approach and for CH_4 with a linear approach. The trends of the experimental results were in accordance with the trends of the thermodynamic calculations for H_2, CH_4 and CO. However, for CO_2 there was a declining trend in the thermodynamic calculations, when 100 vol.-% CO_2 was theoretically used as gasification agent, which doesn´t reflect the results of the experiments. In general, the values of CO were higher and the values of CO_2 and H_2 lower in the thermodynamic equilibrium compared to the experimental results. The content of CH_4 was almost 0 vol.-%$_{db}$ along the increasing CO_2 gasification input. Although, there are quite high deviations between the amount of the product gas components, the thermodynamic calculations provide a good insight, what would theoretically be possible.

Fig. 6 shows the deviation from the RWGS reaction over increasing CO_2 input. Regarding the RWGS reaction, the equilibrium between 827 - 838°C should lie on the side of the products in the thermodynamic equilibrium [16], which was the case for test campaign 1. With increasing CO_2 as gasification agent, the gas composition was shifted towards the educt side. When pure CO_2 was used as gasification agent, the gas composition was completely on the side of the educts, which objected to the predictions of the thermodynamic equilibrium.

One of the reasons for the huge deviations from the thermodynamic equilibrium and the high contents of CO_2 in the product gas of the test campaigns, could be a too low residence time in the gasification reactor. It is well known, that the reaction rate of the Boudouard reaction is much slower than the reaction rate of the RWGS reaction [17]. Longer residence times would improve the conversion efficiency. [18] Due to the inefficient conversion of CO_2, a certain amount of CO_2 maybe took not place on any chemical reaction, which diluted the whole product gas. Additionally, higher temperatures would have also been favorable for the progress of the chemical reactions and thus the conversion efficeincy.

One can conclude from these findings, that using pure CO_2 as gasification agent is not efficient for the biomass gasification process in such temperature ranges. However, using mixtures of steam and CO_2 like in test campaigns 2 and 3, present a promising approach for recycling CO_2 within this process. Additionally, a moderate H_2/CO ratio was generated and the deviation from the chemical equilibrium was close to 0.

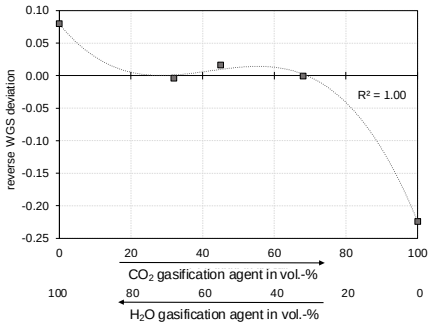

Fig. 5: Change of the deviation from the reverse WGS equilibrium over CO_2 input as gasification agent

3.1 Temperature variation

When fluidizing the gasification reactor with pure CO_2 as gasification agent, a temperature variation from 740 to 840°C was conducted. Beforehand, thermodynamic calculations were carried out as well. The results of these calculations are displayed in **Fig. 6**. In the thermodynamic equilibrium, CO contents of 48 - 55 vol.-%$_{db}$ were possible, while the amount of CO_2 ranged between 23 – 27 vol.-%$_{db}$. The H_2 content was about 23 vol.-%$_{db}$ in average and CH_4 accounted for almost 0 vol.-%$_{db}$.

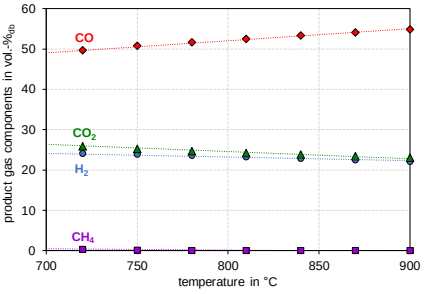

Fig. 6: Change of product gas composition over gasification temperature in the thermodynamic equilibrium

Fig. 6 shows the experimental results of the temperature variation over the gasification temperature TGR_{lower} when pure CO_2 was used as gasification agent. The best fitting trend lines of the experimental results with quite high coefficients of determination were calculated for H_2, CO and CO_2 with an exponential approach and for CH_4 with a linear approach. The trends of CO_2 and CO of the thermodynamic calculations were equal to that of the experimental results, however, the amounts showed quite high deviations. The CO content showed an increase from 23 to 37 vol.-%$_{db}$ and the CO_2 content a decrease from 58 to 40 vol.-%$_{db}$ in the experimental investigations. In contrast to the slightly decreasing trend of H_2 in the thermodynamic calculations along the increasing gasification temperature, the experimental results

showed an increasing course of H_2. CH_4 remained relatively stable with a slight decrease over the increase in temperature during the test campaigns, but accounted for almost 0 vol.-%$_{db}$ in the thermodynamic calculations. In general, there are deviations in the amounts of the product gas components between the thermodynamic calculations and the experimental results, but the trends of CO and CO_2 correspond to the trends of the experimental investigations.

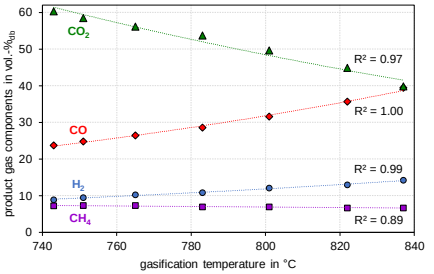

Fig. 7: Change of product gas composition over gasification temperature of test campaign 5

Based on the trends of CO and CO_2 in **Fig. 7**, one can conclude, that higher temperatures, over 840°C would be favorable for using pure CO_2 as gasification agent. At higher temperatures, the RWGS reaction as well as the Boudouard reaction, which both favor the production of CO, would take place to a higher extent (see [16], [18]). **Fig. 8** depicts the deviation from the RWGS reaction equilibrium calculated with **Eq. 6** of the different operating points of the temperature variation. In general, the state of equilibrium was on the side of the educts over the whole temperature range. This could be traced back to too short residence times in the gasificaiotn reactor, which decreased the conversion efficiency of CO_2. This excess CO_2 maybe diluted to whole product gas as explained before. Based on these assumptions, following hypotheses can be proposed: From 740°C to around 780 - 800°C the gas composition was on the educt side. This can be seen in the increasing negative deviation of the RWGS reaction. At around 800°C, the RWGS reaction seemed to be in equilibrium, which was also stated by [19] and [20]. From 800°C, the deviation from the RWGS reaction showed a decreasing course towards the product side. This indicated, that from 800°C, the production of CO and in parallel the conversion of CO_2 was favored. Comparable results for temperatures over 800°C using steam as gasification agent can be found in literature [21].

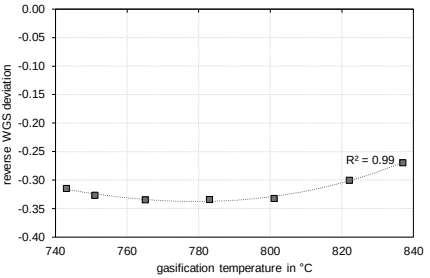

Fig. 8: Change of the deviation from the reverse WGS equilibrium over gasification temperature of test campaign 5

Tab. 5 shows the performance indicating key parameters of validated data with IPSEpro of test campaigns 1 to 5. It is visible, that the CO_2 conversion increased with increasing CO_2 input. Contrarily, the water conversion decreased. This could be explained by the RWGS reaction, where H_2O was formed (see **Eq. 5** in the opposite direction) at temperatures over 800°C. The carbon to CO conversion had a maximum, when the GR was fluidized with pure steam. For this case, the lowest total amount of carbon (C) was introduced into the GR compared to test campaigns 2 to 5, where also the amount of C in the gasification agent accounted to the total C input into the GR. Overall cold gas efficiencies around 70 % were reached for

all test campaigns. The H_2/CO ratio was lowered from 1.49 for pure steam as gasification agent to 0.39 for pure CO_2 gasification. The same declining trend was seen for the lower heating value (LHV). Both trends could be explained the increasing amount of the inert gas CO_2 in the product gas. The gravimetric tar contents of pure steam and pure CO_2 gasification were higher than the one, which was produced when a mixture of steam and CO_2 was used as gasification agent. This could be explained by the combined effect of steam and dry reforming reactions, when a mixture of steam and CO_2 was used as gasification agent [4]. The dust contents were in the range of 0.3 to 1.0 g/m^3_{stp} and are typical values for gasification with olivine as bed material. The char contents were lower, when CO_2 was present in the gasification and higher when only steam was used as gasification agent. This could be explained by a higher amount of fuel, which was introduced into the CR for test campaign 1.

Tab. 5: Performance indicating key parameters

key figure		test campaign				
	unit	1	2	3	4	5
X_{CO2}	kg_{CO2}/kg_{CO2}	0	-0.25	-0.05	0.09	0.29
X_{H2O}	kg_{H2O}/kg_{steam}	0.28	0.18	0.06	-0.16	-0.54
$X_{C\rightarrow CO}$	$kg_{C,CO}/kg_{C,fuel\&fluid}$	0.38	0.34	0.33	0.32	0.34
$\eta_{CG,o}$	%	72	70	67	66	69
H_2/CO	-	1.49	1.04	0.86	0.63	0.39
LHV[a]	MJ/m^3_{stp}	12.7	11.2	10.6	9.2	8.7
grav. tar[b]	g/m^3_{stp}	6.7[c]	n.m.	n.m.	4.1	6.2
dust[b]	g/m^3_{stp}	0.3[c]	n.m.	n.m.	1.0	0.6
char[b]	g/m^3_{stp}	2.4[c]	n.m.	n.m.	1.5	0.5

[a] free of tar and char;
[b] measured by the Test Laboratory for Combustion Plants a TU Wien;
[c] values from another comparable test run with SW as fuel and olivine as bed material;
n.m. not measured;

4. Conclusion and Outlook

The results with CO_2 as gasification agent instead of steam showed, that the product gas was shifted towards higher CO and lower H_2 contents. The stepwise substitution of steam by CO_2 indicated, that it is not beneficial to use pure CO_2 as gasification agent for the biomass gasification process with the investigated process conditions. Mixtures of steam and CO_2 as gasification would be much more efficient regarding the achievement of an appropriate H_2/CO ratio for different syntheses like the dimethylether or the Fischer-Tropsch syntheses. Additionally, the destruction of higher hydrocarbons like tar is also much more efficient when using mixtures of steam and CO_2 as gasification agent. The temperature variation indicated, that higher temperatures, over 840°C would be favorable for pure CO_2 gasification, because the RWGS reaction as well as the Boudouard reaction could take place to a higher extent at higher temperatures. Furthermore higher residence times in the gasification reactor would affect the conversion efficiency of CO_2 in a positive way. In general, the trends of the thermodynamic calculations reflect the trends of the experimental results.

Concluding from the results, the admixture of CO_2 between 0 and 50 vol.-% to the gasification agent mixture is reasonable. An advantageous effect of using CO_2 as gasification or fluidization agent is the possibility to recycle produced CO_2 within the process and therefore reducing CO_2 emissions.
An extended version of this publication would include the presentation of hydrogen balances around the GR and a more detailed discussion of the results. Future investigations could focus on a temperature variation up to temperatures of 900°C. Additionally, an optimized concept of the current reactor design could be carried out for CO_2 gasification in the DFB reactor system.

LIST OF ABBREVIATIONS

C	carbon
CR	combustion reactor
DFB	dual fluidized bed
GR	gasification reactor
LHV	lower heating value
PGY	product gas yield
SW	softwood
vol.-%	volumetric percent
WGS	water gas shift
wt.-%	weight percent

LIST OF SUBSCRIPTS

C	carbon
CO_2	carbon dioxide
CR	combustion reactor
daf	dry and ash-free
db	dry basis
fuel	fuel to gasification reactor
GR	gasification reactor
H_2O	water
PG	product gas
steam	steam input in GR
stp	standard temperature and pressure
th	thermal

LIST OF SYMBOLS

$\dot{m}$	masss flow	kg/s
$\dot{V}_{PG}$	dry volumetric prod. gas flow	m^3/s
X_{CO_2}	CO_2 conversion	%
X_{H_2O}	steam-related water conversion	kg_{H2O}/kg_{H2O}
$X_{C\rightarrow CO}$	Carbon to CO conversion	$kg_{C,CO}/kg_{C,fuel\&fluid}$
$\eta_{CG,o}$	overall cold gas efficiency	%
$\dot{Q}_{loss}$	heat loss	kW
LHV	lower heating value	$MJ/m^3_{stp,db}$

5. Acknowledgements

This work was supported by the European Union´s Horizon 2020 research and innovation programme under grant agreement number 764675 (Heat-to-Fuel).

6. References

[1] Weber G. Production of mixed alcohols using MoS2 catalyst from biomass derived synthesis gas. Doctoral thesis, TU Wien, 2017.

[2] Gruber H, Groß P, Rauch R, Weber G, Loipersböck J, Niel J, et al. Fischer-tropsch Synthesis – Effects of Feedstock Load Changes Regarding Product Quality and Catalyst Attrition. Proc. 25th Eur. Biomass Conf. Exhib. Stock. Sweden, 2017. doi:10.5071/25thEUBCE2017-3AO.9.4.

[3] Hofbauer H. Biomass Gasification for Electricity and Fuels, Large Scale. Encycl. Sustain. Sci. Technol., Springer; 2017, p. 459–78. doi:10.1007/978-1-4614-5820-3.

[4] Mauerhofer AM, Fuchs J, Müller S, Benedikt F, Schmid JC, Hofbauer H. CO_2 gasification in a dual fluidized bed reactor system: Impact on the product gas composition. Fuel 2019.

[5] Fuchs J, Schmid JC, Müller S, Hofbauer H. Dual fluidized bed gasification of biomass with

selective carbon dioxide removal and limestone as bed material: A review. Renew Sustain Energy Rev 2019;107:212–31. doi:10.1016/j.rser.2019.03.013.
[6] Schmid JC. Development of a novel dual fluidized bed gasification system for increased fuel flexibility. TU Wien, doctoral thesis, 2014.
[7] Schmid JC, Pröll T, Kitzler H, Pfeifer C, Hofbauer H. Cold flow model investigations of the countercurrent flow of a dual circulating fluidized bed gasifier. Biomass Convers Biorefinery 2012;2:229–44. doi:10.1007/s13399-012-0035-5.
[8] Mauerhofer AM, Schmid JC, Benedikt F, Fuchs J, Müller S, Hofbauer H. Dual fluidized bed steam gasification: Change of product gas quality along the reactor height. Energy 2019;173:1256–72. doi:10.1016/j.energy.2019.02.025.
[9] Benedikt F, Kuba M, Christian J, Müller S, Hofbauer H. Assessment of correlations between tar and product gas composition in dual fluidized bed steam gasification for online tar prediction. Appl Energy 2020;238:1138–49. doi:10.1016/j.apenergy.2019.01.181.
[10] Müller S, Fuchs J, Schmid JC, Benedikt F, Hofbauer H. Experimental Development of Sorption Enhanced Reforming by the Use of an Advanced Gasification Test Plant. Int J Hydrogen Energy 2017;42:29697–707. doi:10.1016/j.ijhydene.2017.10.119.
[11] Pröll T, Hofbauer H. Development and Application of a Simulation Tool for Biomass Gasification Based Processes. Int J Chem React Eng 2008;6:Article A89. doi:10.2202/1542-6580.1769.
[12] Mauerhofer AM, Müller S, Benedikt F, Fuchs J, Bartik A, Hofbauer H. CO_2 GASIFICATION OF BIOGENIC FUELS IN A DUAL FLUIDIZED BED REACTOR SYSTEM. Biomass Convers Biorefinery 2019. doi:https://doi.org/10.1007/s13399-019-00493-3.
[13] Outokumpu HSC Chemistry Thermochemical Database, ver 6.1 A Roine - Finland: Outokumpu Research Oy, 2018.
[14] Kuba M, Kirnbauer F, Hofbauer H. Influence of coated olivine on the conversion of intermediate products from decomposition of biomass tars during gasification. Biomass Convers Biorefinery 2017;7:11–21. doi:10.1007/s13399-016-0204-z.
[15] Jarungthammachote S, Dutta A. Equilibrium modeling of gasification: Gibbs free energy minimization approach and its application to spouted bed and spout-fluid bed gasifiers. Energy Convers Manag 2008;49:1345–56. doi:10.1016/j.enconman.2008.01.006.
[16] Poboß N. Experimentelle Untersuchung der sorptionsunterstützten Reformierung. University Stuttgart, docotral thesis, 2016.
[17] Ahmed II, Gupta AK. Kinetics of woodchips char gasification with steam and carbon dioxide. Appl Energy 2011;88:1613–9. doi:10.1016/j.apenergy.2010.11.007.
[18] Lahijani P, Alimuddin Z, Mohammadi M, Rahman A. Conversion of the greenhouse gas CO_2 to the fuel gas CO via the Boudouard reaction : A review. Renew Sustain Energy Rev 2015;41:615–32. doi:10.1016/j.rser.2014.08.034.
[19] Aghaalikhani A, Schmid JC, Borello D, Fuchs J, Benedikt F, Hofbauer H, et al. Detailed modelling of biomass steam gasification in a dual fluidized bed gasifier with temperature variation. Renew Energy 2019;143:703–18. doi:10.1016/j.renene.2019.05.022.
[20] Callaghan CA. Kinetics and Catalysis of the Water-Gas-Shift Reaction: A Microkinetic and Graph Theoretic Approach. Worcester Polytechnic Institute, docotral thesis, 2006.
[21] Schmid JC, Benedikt F, Fuchs J, Mauerhofer AM, Müller S, Hofbauer H. Syngas for biorefineries from thermochemical gasification of lignocellulosic fuels and residues - 5 years´ experience with an advanced dual fluidized bed gasifier design. Biomass Convers Biorefinery 2019. doi:doi.org/10.1007/s13399-019-00486-2 REVIEW ARTICLE Syngas.